scientific data

OPEN

DATA DESCRIPTOR

A multi-omics dataset of C57 BL/6J mice regulated function by feed with ε-polylysine

Xuelei Zhang[1,3], Zhenping Hou[2,3], Yuxin Cao[1], Songshan Wang[1], Yong Zhang[1], Jinrong Wang[1] & Duanqin Wu[2] ✉

The proteomic and metabolomic differences in mice fed ε-polylysine were detected by high-throughput sequencing and screening. The effects of ε-polylysine on the proteome and metabolomics of C57 BL/6 J mice were studied. DIA proteome sequencing and liquid chromatography-mass spectrometry (LC-MS) were used to compare ε-polylysine-modified mouse proteome and metabolome. In this study, we analyzed the regulatory effects of ε-polysine on glycerophospholipid metabolism, glutathione metabolism, and ABC transporters pathways. The sequencing data and LC-MS/MS raw data of samples are stored in MetaboLights and ProteomeXchange databases for efficient reuse and to explore the differences in metabolism and protein expression among mice fed with different levels of ε-polylysine, aiming to screen for critical proteins and differential metabolites in valuable regulatory pathways.

Background & Summary

ε-Polylysine is a homopolymer comprising 25–35 lysine molecules. It was originally found to be produced by Streptomyces No. 346[1]. In the ε-polylysine polypeptide sequence with a total length of 30, the 4–24 L-Lys residues tend to form α-helix in the secondary structure sequence, accounting for 86.7%, and the other 13.3% residues tend to form rings. Thus, ε-polylysine ingestion shows no toxic side effects due to its secondary structure units and has good biocompatibility. And the small portion of ε-polylysine used by the body can be hydrolyzed into small amino acids via hydrolysis or C degradation-based enzyme catalysis; these amino acids are absorbed or metabolized via endocytosis into cells for protein synthesis. The use of a small amount of ε-polylysine can exert a potent bacteriostatic effect, which reduces the cost in practical applications.

ε-Polylysine is widely recognized as a food additive owing to its characters. ε-Polylysine is recognized as GRAS by the U.S. Food and Drug Administration (FDA) and can be used as an antimicrobial agent in the food industry. At present, Japan, South Korea, the United States, China and other countries allow the use of biological preservatives in the food industry. ε-polylysine has a strong inhibitory effect on many foodborne pathogens such as *Escherichia coli* O157:H7, *Listeria monocytogenes* and *Staphylococcus aureus*[2–4]. ε-Polylysine can be used not only alone, but often in combination with other food additives, such as glycine, ethanol, and acetic acid, which may reduce the amount of each additive used in food production[5]. These combinations contained the ε-polylysine/chitosan nanofibers[6], ε-polylysine/glucan[5,7] and so on, which could significantly behave as potent antibacterial material in food packaging and preservation systems and couple with as a bifunctional food additive with emulsifying and antimicrobial properties. Furthermore, ε-polylysine has a wide range of applications in drug discovery and development, including drug delivery, gene vectors, diagnostic imaging, diagnostics, biosensors, and specialty cancer therapies[8–11].

Despite the extensive applications of ε-polylysine in food and medicine, research on its metabolism and nutritional impact within the body remains scarce. Focusing on the liver, a crucial metabolic organ, previous studies have suggested that ε-polylysine exerts a significant influence on lipid and lipoprotein metabolism[12]. Metabolomics investigated the composition and alterations of metabolites, revealing the holistic metabolic responses and dynamic changes in C57 BL/6 J mice under varying levels of ε-polylysine supplementation. Meanwhile, proteomics techniques could elucidate the impact of ε-polylysine on protein expression in C57 BL/6 J mice, as proteins were integral to metabolism and other cellular functions. Therefore, this

[1]School of Biological Engineering, Henan University of technology, Zhengzhou, China. [2]Institute of Bast Fiber Crops, Chinese Academy of Agricultural Sciences, Changsha, China. [3]These authors contributed equally: Xuelei Zhang, Zhenping Hou. ✉e-mail: wuduanqin@caas.cn

study employed a systematic approach, combining data-independent acquisition (DIA) proteomics and liquid chromatography-tandem mass spectrometry (LC-MS/MS), to comprehensively compare the alterations in hepatic metabolomics and proteomics profiles of mice fed with different doses of ε-polylysine. This analysis validated the regulatory effects of ε-polylysine on target proteins involved in metabolic pathways. All data generated were deposited in the iProX and metabolights databases.

The public availability of this dataset facilitates advancements in research on the role of food additives in nutritional metabolism and other functional regulations in animals. It enables repetitive or combined analyses of multi-omics data, as well as comparisons across different studies in proteomics and metabolomics. This dataset offers versatility and synergy for analysis from multiple angles. Firstly, it showcases the alterations in hepatic proteomics and metabolomics profiles of mice induced by ε-polylysine, facilitating an in-depth analysis of its effects. Secondly, it aids in elucidating the regulatory mechanisms of differential metabolic pathways in the liver, encompassing glycerophospholipid metabolism, glutathione metabolism, and ABC transporter pathways. Thirdly, it facilitates the prediction of organismic responses to ε-polylysine and the identification of key proteins and metabolites. This study explores the potential applications of ε-polylysine, providing a reference for its utilization as a multifunctional additive.

Methods

Animals and specimen collection. We chose 80 3-week-old specific pathogen-free (SPF) C57 BL/6 J male mice (9.35 ± 1.13 g), which were randomly assigned to four groups. One week after the adaptation period, we started feeding different groups of mice with different supplemental doses of ε-polylysine. Mice in each group (n = 20) were fed the same diet (AIN-76A) supplemented with 0, 300, 600, and 1,200 mg/kg ε-polylysine, respectively. C57 mice were maintained in the same condition, under 12:12 h light/dark and free access to feed and water. The entire trial period on mice was from 3-week-old to 11-week-old. At end of the experiment, the mice were anesthetized and euthanized, and liver samples were harvested. The samples were snap-freezing in liquid nitrogen and transferred to −80 °C refrigerator.

Metabolomics analysis. Liquid chromatography-mass spectrometry (LC-MS) sample preparation and analysis. After grinding, 30 mg of liver sample, 20 μL of L-2-chlorophenylalanine (0.3 mg/mL; Hengchuang, Shanghai, China) and 400 μL extraction solvent containing methanol/water (4/1, v/v) (CNW Technologies GmbH, Dusseldorf, Germany) were added into a 1.5 mL Eppendorf tube which was stored at −80 °C for 2 min, and the sample was then ground at 60 Hz for 2 min. The samples were ultrasonicated at 25–28 °C for 10 min and then stored at −20 °C for 30 min. The centrifuge was set at 13,000 rpm and 4 °C for 15 min, and 300 mL of supernatant was dried. To each sample, 400 μL methanol and water (1/4, v/v) were added, vortexed for 30 seconds, and then placed at 4 °C for 2 min. 5 min at 4 °C and 13,000 rpm were used for centrifuging samples. Subsequently, 150 μL of supernatants from each tube was collected using crystal syringes, filtered through 0.22 μm microfilters, and transferred to LC vials. The vials were stored at −80 °C until LC-MS analysis.

Metabolic profiling was performed using the AB ExionLc system (AB SCIEX, Framingham, MA, USA) coupled with an AB SCIEX Triple TOF 6600 System (AB SCIEX). An ACQUITY UPLC HSS T3 column (1.8 μm, 2.1 × 100 mm) were employed in both positive and negative modes. The injection volume was 5 μL. The binary gradient elution system consisted of (A) water (containing 0.1% formic acid, v/v) and (B) acetonitrile (containing 0.1% formic acid, v/v) and separation was achieved using the following gradient: 0 min, 5% B; 2 min, 20% B; 4 min, 25% B; 9 min, 60% B; 14 min, 100% B; 16 min, 100% B; 16.1 min, 5% B and 18.1 min, 5% B. The flow rate was 0.35 mL/min and column temperature were 45°C. All the samples were kept at 4°C during the analysis. Data acquisition was performed in full scan mode (m/z ranges from 100 to 1,000) combined with IDA mode. Parameters of mass spectrometry were as follows: Ion source temperature, 550 °C (+) and 550 °C (−); ion spray voltage, 5,500 V (+) and 4,500 V (−); curtain gas of 35 PSI; nebulizer gas of 55 PSI; auxiliary gas of 55 PSI; declustering potential, 80 V (+) and 80 V (−); collision energy, 10 eV (+) and 10 eV (−); and interface heater temperature, 550 °C (+) and 550 °C (−). For IDA analysis, the peptide fragments of each sample after enzymatic digestion were collected separately, and the scanning range was set to 350–1250 m/z and the isolation window was 26 m/z. The collision energy was 35 eV. The DIA mass spectrum conditions, chromatographic conditions and key parameters of data analysis were shown in the Tables 1–3. In the metabolomics data, all samples were mixed in equal amounts as QC samples. During the mass spectrometry process, a QC sample was inserted into every 8 formal samples. The QC sample was used to evaluate the stability of the system mass spectrometry platform during the entire experiment. The QCs were injected at regular intervals throughout the analytical run to provide a set of data from which repeatability can be assessed.

Data preprocessing and statistical analysis. Progenesis QI V2.3 (Nonlinear Dynamics, Newcastle, United Kingdom) was used to process the original LC-MS data, and R was used to perform principal component analysis. For the extracted data, the ion bees with missing values (0 value) > 50% in the group are deleted, and the 0 value is replaced with half of the minimum value. The qualitative compounds are screened according to the compound qualitative result score (Sc0r). The screening standard is 30 points (out of 60 points). The qualitative results below 30 points are considered inaccurate and deleted. Data were filtered based on PSM concentration and 1% false discovery rate (FDR) to reduce false positive results. Untargeted metabolomics workflow for identification using mzCloud (ddMS2), ChemSpider(formula or exact), and Kyoto Encyclopedia of Genes and Genomes (KEGG) pathway was used to process the original data. The identification of compounds was based on accurate mass number, secondary debris and isotopic distribution, and qualitative analysis was performed using The Human Metabolome Database (HMDB), Lipidmaps (v2.3), METLIN Database and self-built database. In order to distinguish the metabolites among the groups, OPLS-DA (Orthogonal Partial Least Squares Discriminant Analysis) was performed. Seven-fold cross-validation was performed along with 200 Response

Items	Full MS	MS2
Resolution	120000	30000
AGC target	3e6	1e6
Maximum injection time	100 ms	Auto
Scan range	350–1250 m/z	—
Isolation window	—	26 m/z
Normalized Collision Energy	—	28

Table 1. DIA Mass spectrum conditions.

Time (min)	Gradient
0	5% B
82	44% B
84	90% B
90	90% B

Table 2. DIA Chromatographic conditions.

Items	Para.
Precursor Qvalue cutoff	0.05
Protein Qvalue cutoff	0.05
Normalization Strategy	Local Normalization
Quantity MS-Level	MS2

Table 3. DIA Key parameters of data analysis.

Permutation Testing. For each variable, VIP values were used to rank its overall contribution to group discrimination. Students' t-tests were used to further verify whether there were significant differences between groups in metabolites. The differential metabolites were selected based on VIP values > 1.0 and P-values < 0.05.

Proteomics analysis. Protein extraction and concentration determination. Liver samples, 300 μL sodium dodecyl sulphate (SDS) Lysis Buffer (Biyuntian, Shanghai, China), and protease inhibitor PMSF (Amresco, Fountain Parkway Solon, OH, USA) were added to 1.5 mL Eppendorf tubes to a final concentration of 1 mM. Ultrasonic crushing in ice was performed for 3 min (power, 80 W). At ambient temperature, the solution was centrifuged at 12,000 rpm for 10 min and the supernatant collected. BCA kits (Thermo Fisher Scientific, China) were used to quantify total protein. Subsequently, 10 μg protein was extracted from each sample and separated via 12% SDS-polyacrylamide gel electrophoresis. After separation, the gel was stained using Coomassie Brilliant Blue staining method as described by Candiano *et al.*[13]. The dyed gel was scanned using an ImageScanner scanner in full color mode with an optical density value of 300 dpi.

Trypsin enzymolysis and desalting of peptides. Briefly, 50 μg protein from each sample was prepared and different groups of samples were diluted and adjusted to the same concentration and volume with lysate. Dithiothreitol (DTT) (Shenggong, Shanghai, China) was added to the aforementioned protein solution to make the final concentration of DTT at 4.5 mM, following mixing and incubation at 55 °C for 30 min. The corresponding volume of iodoacetamide was added to make the final concentration of 9 mM, after which the solution was mixed and placed at room temperature away from light for 15 min. Subsequently, 6 times the volume of acetone to the above solution were added to precipitate proteins and the solution was left at −20 °C for more than 4 h or overnight. The precipitates were collected by centrifugation at 8,000 rpm at 4 °C for 10 min, and acetone was volatilized for 2–3 min. Subsequently, 100 μL TEAB2 was added to resolubilize the precipitate. Next, 1/50 sample mass of 1 mg/mL trypsin-TPCK (Hualishi, Beijing, China) was added following overnight digestion at 37 °C. Phosphoric acid was added to adjust the PH to approximately pH 3 and enzymatic hydrolysis was terminated. Salt was removed from the peptides including activation of a column using 200 μL methanol, which was repeated twice. The column was balanced using 200 μL pure water, which was repeated twice. Subsequently, 50–500 μL sample was loaded, vacuum was adjusted, and droplet speed was maintained at 1 mL/min (approximately 1 droplet/s), which was repeated once. The column was washed with 200 μL 5% methanol, which was repeated twice. The peptide was eluted using 150 μL methanol, which was repeated twice for a total of three times to obtain 450 μL eluent, followed by vacuum drying.

LC-MS/MS and bioinformatics analysis. A Q Exactive HF mass spectrometer coupled to an EASY-1200 nLC system (Thermo Fisher Scientific, Waltham, MA, USA) was used to perform LC-MS/MS analysis, which the injection volume was 300 ng. Data-independent acquisition (DIA) raw data were processed using Spectronaut Pulsar software. For reliable protein analysis and data quality control in proteomics, the raw data is obtained

iRT Peptide Sequence	Coefficient of Variation (CV)
ADVTPADFSEWSK	0.25%
GAGSSEPVTGLDAK	0.43%
GTFIIDPAAVIR	0.24%
GTFIIDPGGVIR	0.23%
LFLQFGAQGSPFLK	0.24%
LGGNEQVTR	1.61%
TPVISGGPYEYR	0.33%
TPVITGAPYEYR	0.32%
VEATFGVDESNAK	0.38%
YILAGVENSK	0.35%

Table 4. iRT coefficient of variation.

Items	Full MS	MS2
Resolution	120000	30000
AGC target	3e6	2e5
Maximum injection time	100 ms	80 ms
Scan range	350–1650 mz	200–2000 m/z
Isolation window	—	1.4 m/z
Normalized Collision Energy	—	27

Table 5. DDA Mass spectrum conditions.

Time(min)	Gradient
0	5%B
82	44%B
84	90%B
90	90%B

Table 6. DDA Chromatographic conditions.

Items	Para.
Missed cleavage	2
Fixed modification	Carbamidomethyl(C)
Variable modification	Oxidation (M)
Enzyme	Trypsin/P
Protein FDR Cut Off	0.01
Peptide FDR Cut Off	0.01
PSM FDR Cut Off	0.01
Database	uniprot-reviewed Mus musculus(Mouse)

Table 7. DDA Chromatographic conditions.

by database retrieval, and the proteins with expression values $\geq$ 50% of any group of samples are retained. The missing values s50% of the proteins are filled with the mean of the samples in the same group, and the reliable proteins are obtained by Median Normalization and log2 logarithmic transformation. We used iRT internal standards for quality control of protein data, and observed the reliability and stability of data during mass spectrometry acquisition by evaluating its CV (coefficient of variation). the iRT coefficient of variation was shown in Table 4. The scanning parameters of mass spectra are shown in the Table 5. The liquid phase elution gradient is shown in the Table 6. The flow rate was 300 nL/min with 0.1% FA aqueous solution for buffer A and 0.1% FAW 80% ACN/ 20% water for buffer B. The purpose of this operation is to match the spectra output by mass spectrometry with the theoretical spectra generated by the aSa library, to convert the machine signal into peptide and protein sequence information, and then to combine sequence information, peptide retention time, fragmentation Sheet ion information was used to establish the spectrum library for subsequent DA analysis. The original files of LC-MS/MS were imported into Spectronaut Pulsar software for library searching and library building. The main parameters are shown in the Table 7. For the identified proteins, each annotation

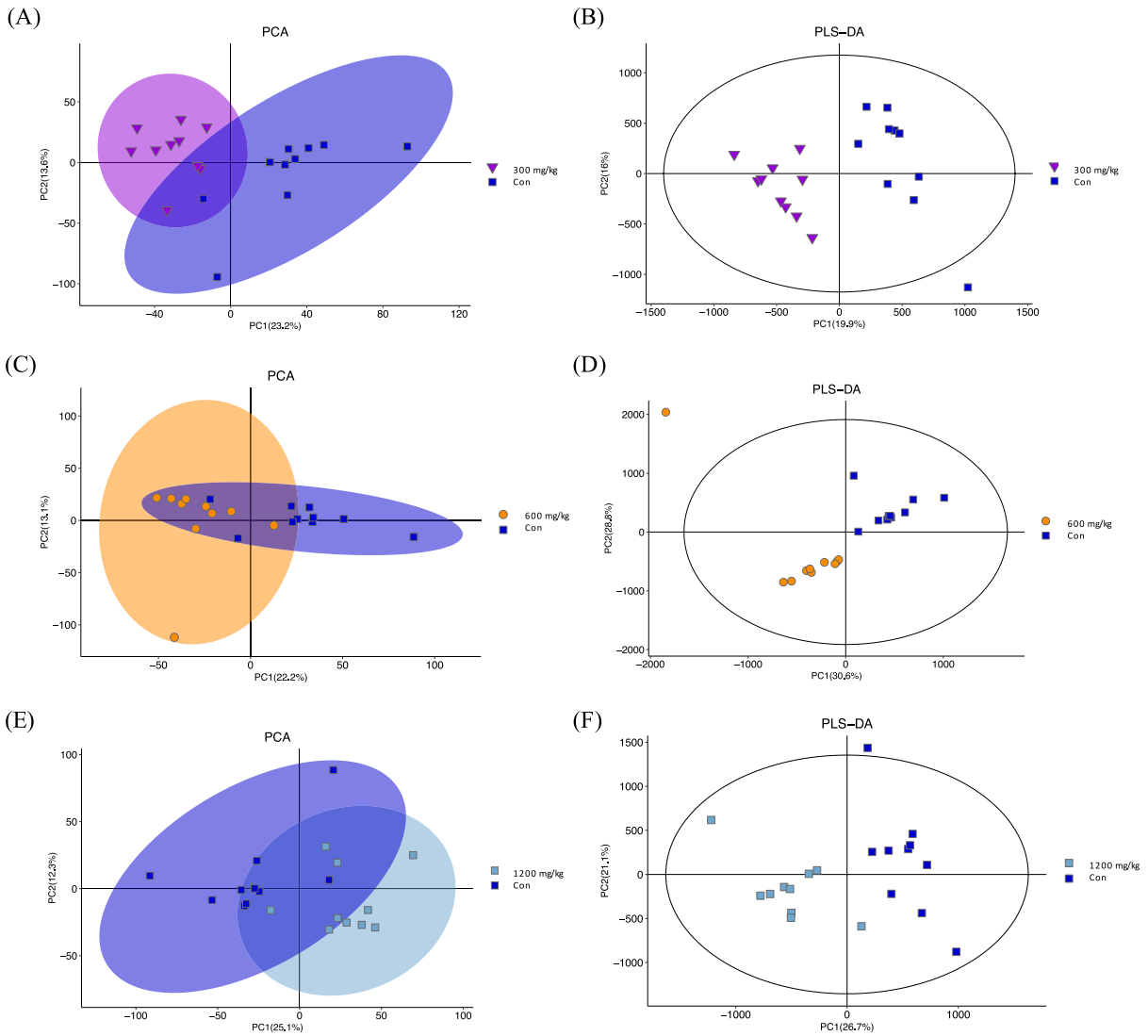

Fig. 1 (**A**) PCA analysis between control and 300 mg/kg ε-polylysine groups. (**B**) Clustering analysis of PLS-DA of the control and 300 mg/kg ε-polylysine groups. (**C**) PCA analysis between the control and 600 mg/kg ε-polylysine groups. (**D**) Clustering analysis of PLS-DA of the control and 600 mg/kg ε-polylysine groups. (**E**) PCA analysis between the control and 1,200 mg/kg ε-polylysine groups. (**F**) Clustering analysis of PLS-DA of the control and 1,200 mg/kg ε-polylysine groups.

information was extracted based on Uniprot, KEGG, GO, KOG/COG and other databases, and protein functions were mined. After obtaining the differentially expressed proteins, GO/KEGG enrichment analysis was performed on the differentially expressed proteins to describe their functions. GO/KEGG functional enrichment analysis method: species proteins were used as the background list, and the list of differential proteins was used as the candidate list filtered from the background list. Hypergeometric distribution test was used to calculate the p value representing whether functional sets were significantly enriched in the list of differential proteins, and then the p value was corrected by Benjamini & Hochberg multiple tests to obtain FDR.

Data Records

The raw LC-MS/MS data files from the non-targeted metabolomic analysis of mouse liver tissues treated with various doses of polylysine have been uploaded to the MMTBLS4273 database (http://www.ebi.ac.uk/metabolights)[14]. Additionally, the original files of liver proteomics data have been deposited in the ProteomeXchange PXD055010 database (https://www.iprox.cn/)[15].

Technical Validation

Metabolic profiles of liver in C57 BL/6 J mice by ε-polylysine.

Quantitative and qualitative analysis. The extracted data, the missing value in the group and the qualitative result score of the compound were combined to screen the qualitatively obtained compounds, and finally the positive and negative ion data were combined into a data matrix. We found that more compounds were

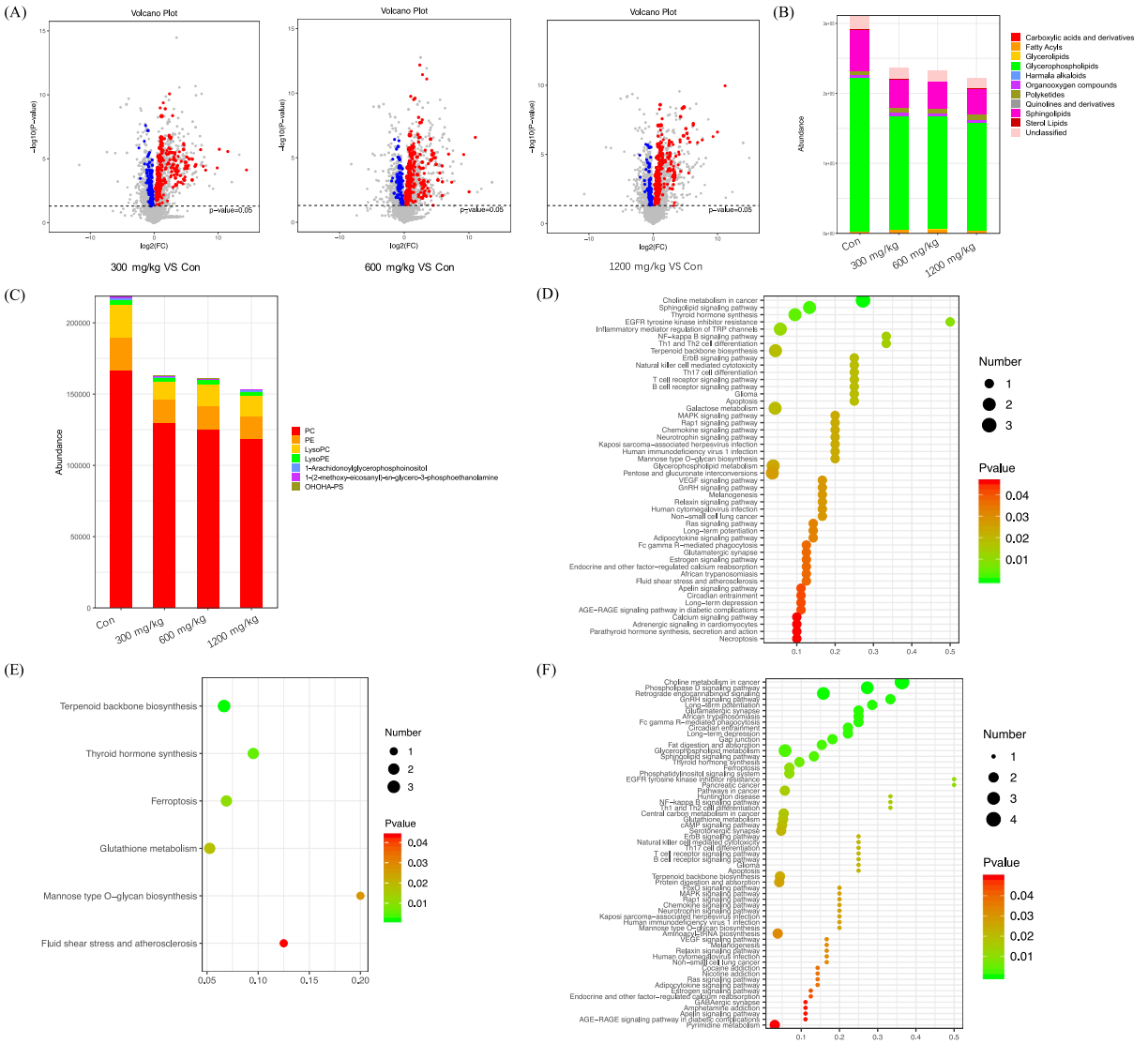

Fig. 2 (**A**) Volcano plot comparing the experimental groups with the control group. The abscissa of the volcano chart is log2 (FC), and the farther the value is from 0, the greater is the difference. The right side indicates upregulation and the left side indicates downregulation. The ordinate is -log10 (p-value). The farther the ordinate is from 0, the greater is the difference. The blue and red dots indicate downregulated and upregulated differentially expressed metabolites, respectively, and the gray dots indicate non-significant differentially expressed metabolites. (**B**) Comparison of the abundance of major metabolite classifications. (**C**) Comparison of the abundance of glycerophospholipids. (**D**) Pathways in the control and 300 mg/kg ε-polylysine groups. (**E**) Pathways in the control and 600 mg/kg ε-polylysine groups. (**F**) Pathways in the control and 1,200 mg/kg ε-polylysine groups.

detected in positive mode than in negative mode. The data contains ions with retention time and mass to charge ratio ID, metabolites name, class, formula and peak integration values, etc. A total of 6369 metabolites were identified, of which 693 metabolites were annotated using the HMDB database, 2455 metabolites were annotated using the LIPID MAPS database, 711 metabolites were annotated using the METLIN database.

Multivariate statistical analysis. Multivariate statistical analysis used unsupervised principal component analysis (PCA) to observe the overall distribution among samples and the stability of the entire analysis process. And multivariate statistical analysis used supervised partial least square analysis (PLS-DA) and orthogonal partial least square analysis (OPLS-DA) to distinguish the overall differences in metabolic profiles between groups and find the differences in metabolites between groups. As shown in Fig. 1, all samples in each PCA score plot were within the 95% confidence ellipse. In 300 mg/kg group compared with the control group, PC1 accounted for 13.6% and PC2 accounted for 23.2% (Fig. 1A). PLS-DA results of liver samples between 300 mg/kg group and control groups were presented in Fig. 1B. PC1 accounted for 13.1% and PC2 accounted for 22.2% between the 600 mg/kg and control group (Fig. 1C), and PLS-DA results was showed in Fig. 1D. PC1 accounted for 12.3%

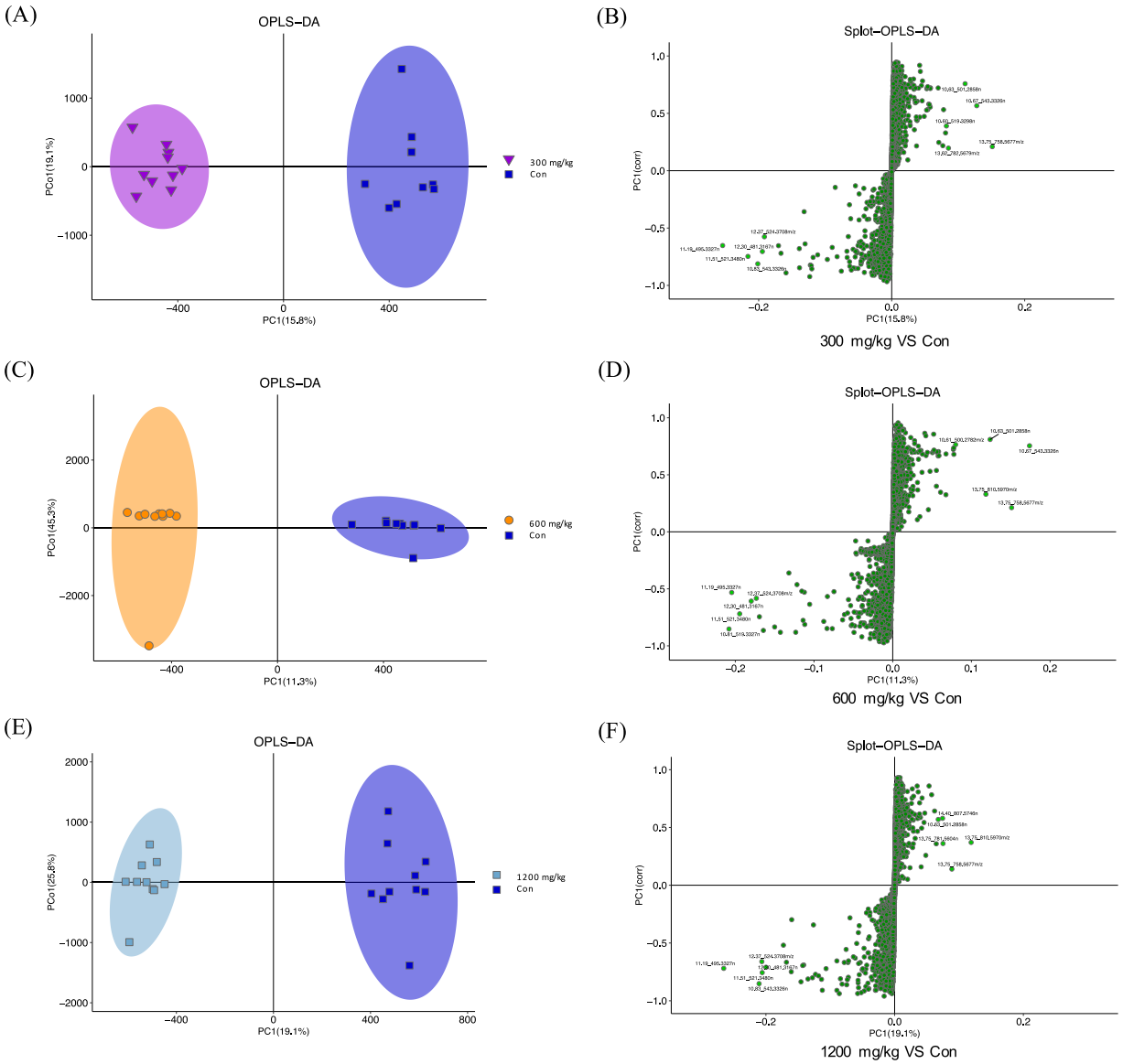

Fig. 3 (**A**) Clustering analysis of OPLS-DA of the control and 300 mg/kg ε-polylysine groups. (**B**) Splot-OPLS-DA analysis of the control and 300 mg/kg ε-polylysine groups. (**C**) Clustering analysis of OPLS-DA of the control and 600 mg/kg ε-polylysine groups. (**D**) Splot-OPLS-DA analysis of the control and 600 mg/kg ε-polylysine groups. (**E**) Clustering analysis of OPLS-DA of the control and 1,200 mg/kg ε-polylysine groups. (**F**) Splot-OPLS-DA analysis of the control and 1,200 mg/kg ε-polylysine groups. The abscissa of the Splot plot is the characteristic value of the influence of metabolites on the comparison group, and the ordinate is the correlation between the sample score and metabolites. The closer the metabolites are to the upper right and lower left corner, the more significant the difference.

and PC2 accounted for 25.1% between the 1,200 mg/kg and control group (Fig. 1E), PLS-DA results as shown in Fig. 1F. OPLS-DA was modified on the basis of PLS-DA to maximize the difference between different groups within the model. The OPLS-DA results were shown in Fig. 3A,C,E. Otherwise, Splot OPLS DA showed the characteristic values of the effects of metabolites on the comparison group and the correlation between sample scores and metabolites. We chose 10 of the more significant the difference, which was closer the metabolites that were to the upper right and lower left corner (Fig. 3B,D,F). Based on these findings, the distribution results showed that there were significant differences among ε-polylysine groups and control group.

Screening and classification of metabolites. We provided the comparison of metabolites among ε-polylysine groups and control group. The volcano plot was used to visualize the P-value, VIP and Fold change value, and the up-regulated and down-regulated differential metabolites were screened out as shown in the Fig. 2A,B,C. Compared with the control group, 227, 212, 211 differentially accumulated metabolites were obtained in 300, 600 and 1200 mg/kg groups, respectively. The results showed that the top 10 classifications of different metabolites were carboxylic acids and derivatives, fatty acyls, glycerolipids, glycerophospholipids, harmala

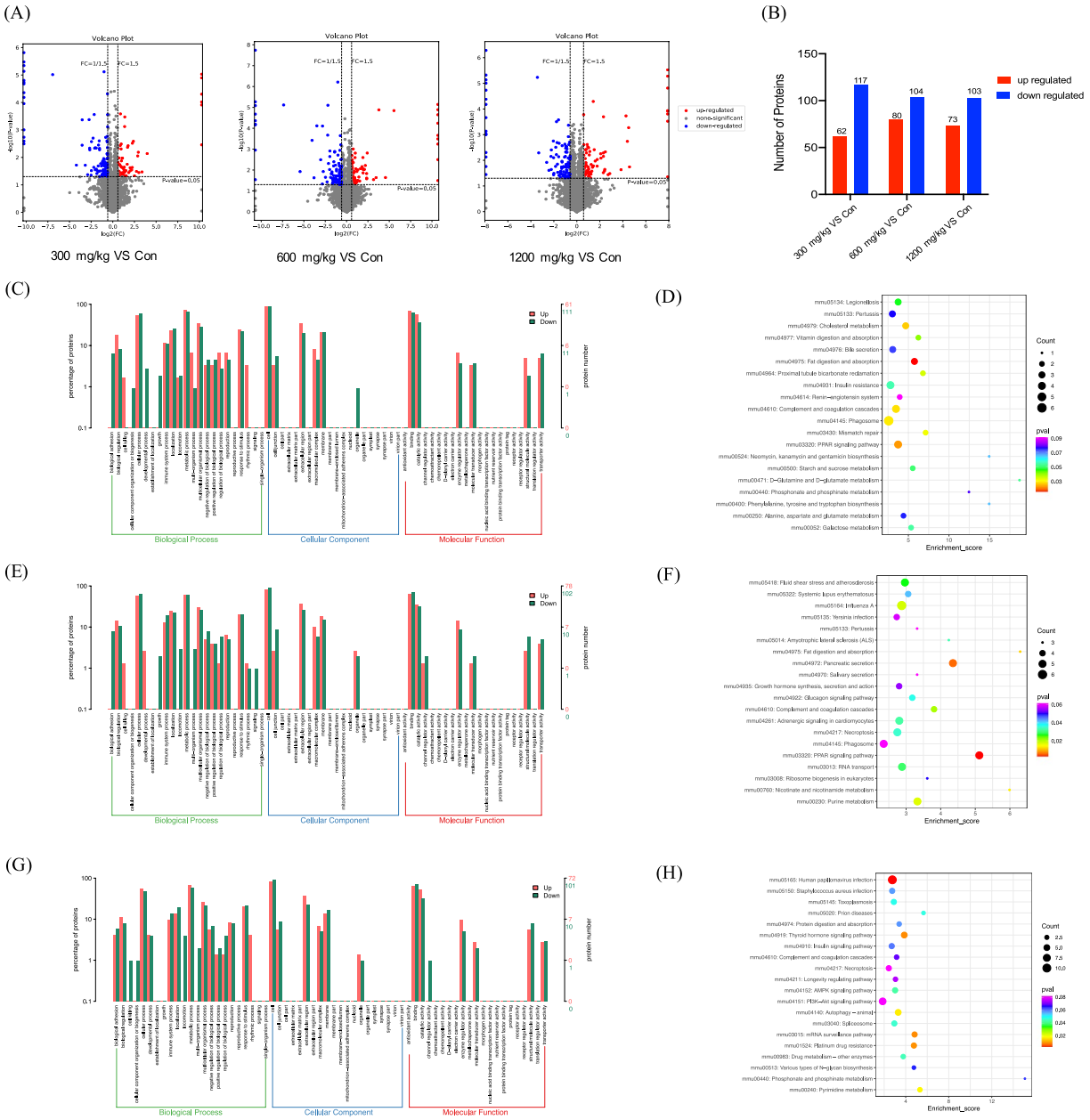

Fig. 4 (**A**) Volcano plot comparing the experimental groups with the control group. The abscissa of the volcano chart is log2 (FC), and the farther the value is from 0, the greater is the difference. The right side indicates upregulation and the left side indicates downregulation. The ordinate is -log10 (p-value). The farther the ordinate is from 0, the greater is the difference. The blue and red dots indicate downregulated and upregulated differentially expressed proteins, respectively, and the gray dots indicate non-significant differentially expressed proteins. (**B**) Number of up-and down-regulated proteins between the ε-polylysine groups and control group. (**C**) Functional annotation of differentially abundant proteins between 300 mg/kg group and control group. (**D**) KEGG pathway enrichment statistics of differentially abundant proteins between 300 mg/kg group and control group. (**E**) Functional annotation of differentially abundant proteins between 600 mg/kg group and control group. (**F**) KEGG pathway enrichment statistics of differentially abundant proteins between 600 mg/kg group and control group. (**G**) Functional annotation of differentially abundant proteins between 1,200 mg/kg group and control group. (H)KEGG pathway enrichment statistics of differentially abundant proteins between 1,200 mg/kg group and control group.

alkaloids, organooxygen compounds, polyketides, quinolines and derivatives, sphingolipids and sterol lipids (Fig. 2D). The abundance of organooxygen compounds, fatty acids, and polyketide metabolites was increased after ε-polylysine treatment; however, the abundance of other metabolites including glycerophospholipids, glycerolipids, sphingolipids, sterol lipids, and carboxylic acids was decreased after ε-polylysine treatment. We further

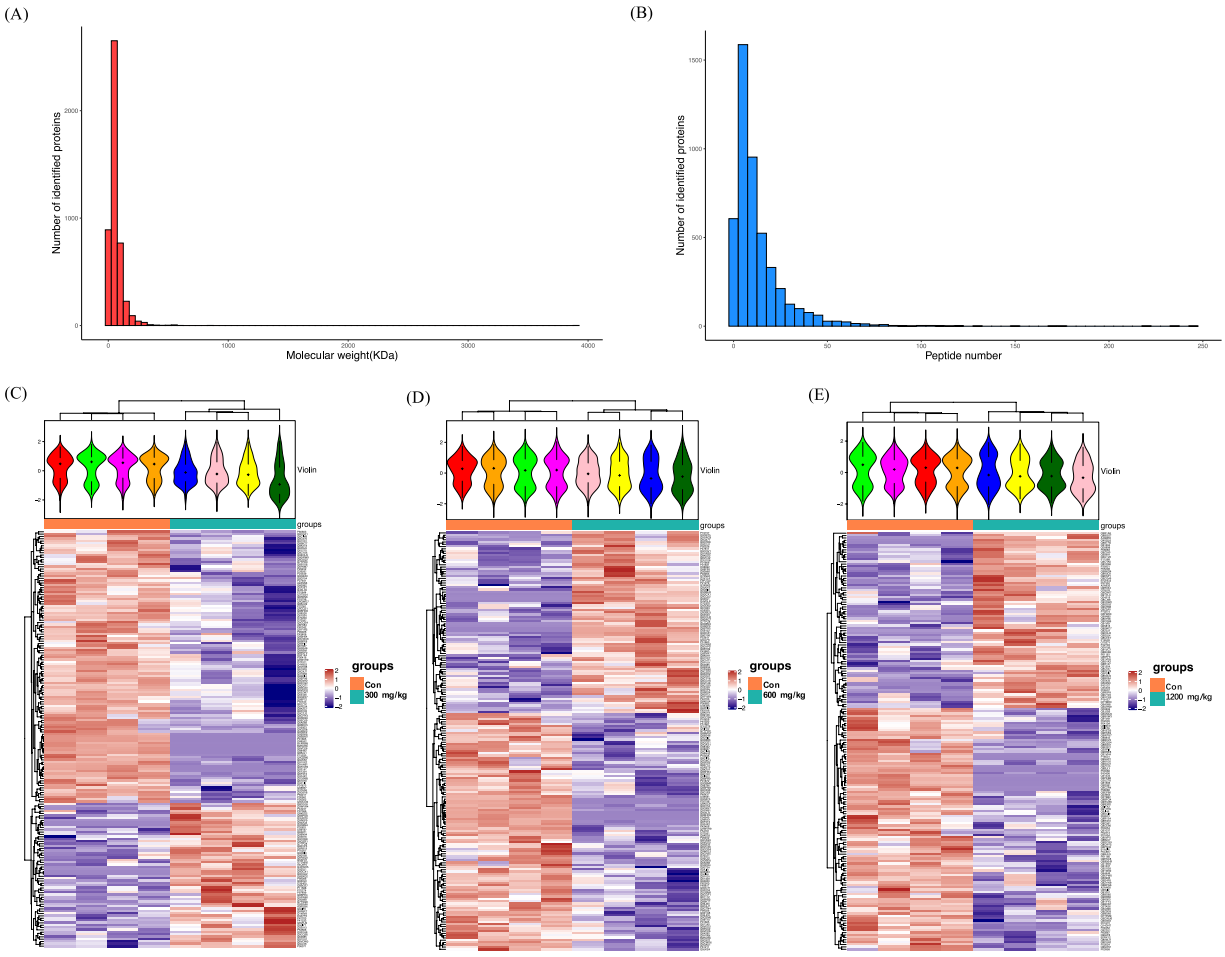

Fig. 5 (**A**) The number of proteins corresponding to different molecular weights. (**B**) The number distribution of peptide corresponding to qualitative protein. (**C**) Heatmap clustering the differential proteins shared between control and 300 mg/kg groups. (**D**) Heatmap clustering the differential proteins shared between control and 600 mg/kg groups. (**E**) Heatmap clustering the differential proteins shared between control and 1,200 mg/kg groups.

examined the taxonomic composition of the glycerophospholipid metabolites and found that PC, PE, and LysoPC represented the domain metabolites among all groups (Fig. 2E).

Metabolic pathway enrichment analysis. Differentially accumulated metabolites with enrichment pathway annotations were shown. We used the KEGG database to match metabolic pathways of metabolites, and conducted enrichment analysis of different metabolic pathways with P-values less than 0.05 to more intuitively analyze the effects of ε-polylysine on mouse metabolism. Metabolite differences significantly enrich metabolic pathways, including glutathione metabolism, glycerophospholipid metabolism, choline metabolism in cancer and so on (Fig. 2F,G,H).

Proteomic analysis of liver in C57 BL/6 J mice by ε-polylysine. *Protein identification and analysis.* We obtained 6671 proteins in the DDA spectrum library through DIA experiment identification. 4726 original proteins and 4712 trusted proteins were identified through DIA identification. Most of the molecular weights of proteins were concentrated below 300 kDa (Fig. 3A). In this study, 63429 peptides were identified, among which 61287 peptides were annotated, and the number of identified protein peptides was mainly concentrated below 50 peptides (Fig. 3B). Compared different dosage of ε-polylysine group with the control group, the protein clustering heat map were shown in Fig. 3C,D,E. A total of 420 differentially expressed proteins between groups were identified and quantified. A Volcano plot of proteins was generated that visualized the overall protein change (Fig. 4A). The number of unique up-as well as down-regulated proteins compared ε-polylysine groups with control group. Proteins with abundance differences were summarized. Of these, 179 proteins (upregulated, 62; downregulated, 117) were found when comparing 300 mg/kg group with the control group; 184 proteins (upregulated, 80; downregulated 104) were found between 600 mg/kg group and control group; 176 proteins (upregulated, 73; downregulated, 103) were found between 1,200 mg/kg group and control group (Fig. 4B). Compared with the control group, the number of proteins with abundance differences in the ε-polylysine groups was more down-regulated

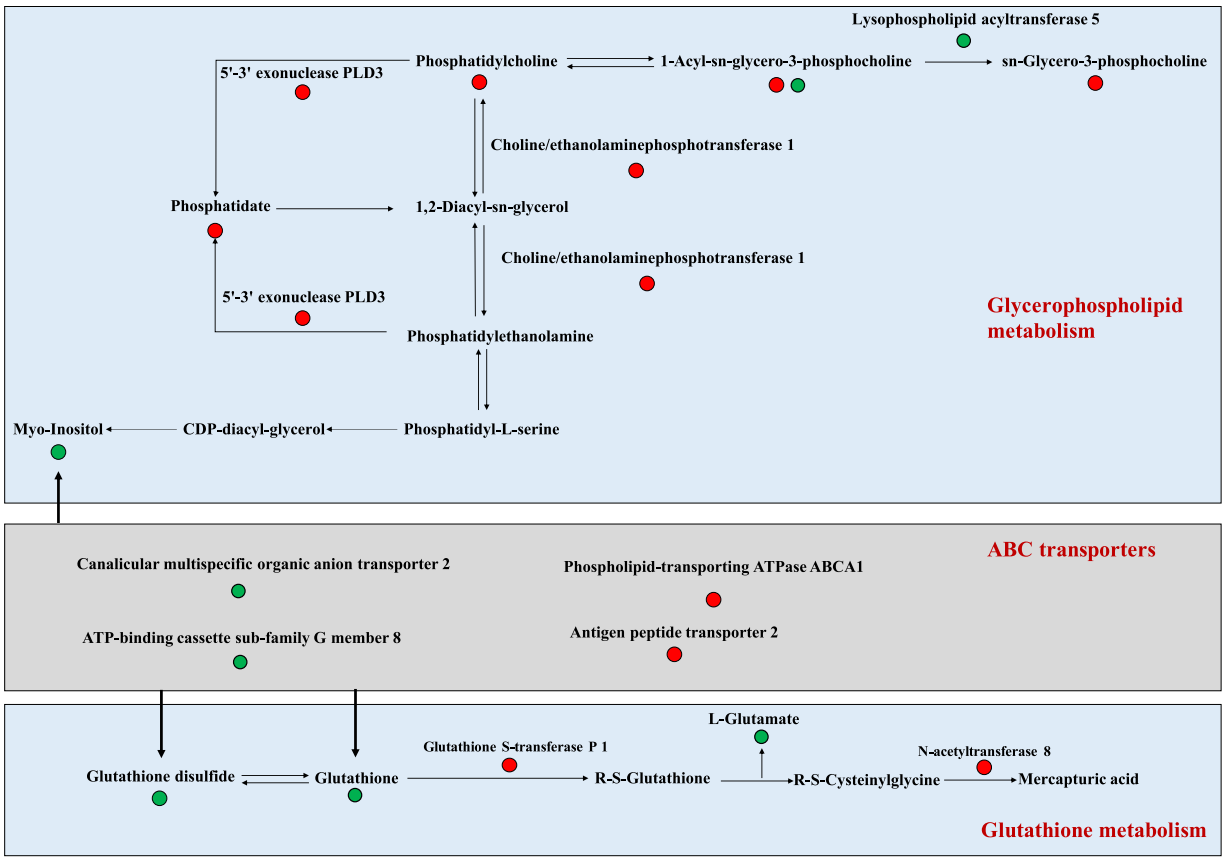

Fig. 6 Changes in the glutathione metabolism, glycerophospholipid metabolism and ABC transporters pathways regulated by ε-polylysine; red indicates up-regulation, while green indicates down-regulation.

than up-regulated. This indicated that ε-polylysine have a complex regulation of nutrient metabolic pathway in C57BL/6J mice.

Proteomic hierarchical cluster and functional classification. Based on the results of GO enrichment analysis, the differentially abundant proteins were classified into biological process, cellular component, and molecular function. With regarded to the GO annotation of 300 mg/kg group vs control group, 61 up- and 111 down-regulated proteins were assigned to 40 biological process categories, 92 cellular component categories (mainly mitochondrion, endoplasmic reticulum, perinuclear region of cytoplasm, mitochondrial outer membrane and extracellular exosome) and 58 molecular function categories (mainly ATP binding and ATPase activity) (Fig. 4C). Compared 600 mg/kg group with control group, 78 up- and 102 down-regulated proteins were assigned to 49 biological process categories (mainly negative regulation of viral genome replication, negative regulation of protein ubiquitination, negative regulation of transcription, DNA-templated and complement activation, classical pathway), 155 cellular component categories (mainly cytoplasm, cytosol, perinuclear region of cytoplasm, extracellular exosome and lysosomal membrane) and 69 molecular function categories (mainly RNA binding, protein heterodimerization activity, GTPase activator activity, metal ion binding and serine-type endopeptidase activity) (Fig. 4E). In addition, 72 up- and 101 down-regulated proteins were assigned to 49 biological process categories (mainly positive regulation of autophagy, glucose homeostasis and negative regulation of MAP kinase activity), 159 cellular component categories (mainly cytoplasm, mitochondrion, keratin filament, extracellular exosome, cytosol, extracellular space and endoplasmic reticulum membrane) and 47 molecular function categories (mainly protein heterodimerization activity, structural constituent of cytoskeleton and mRNA 3′-UTR binding) with regards to the GO annotation of 1200 mg/kg group vs control group (Fig. 4G). According to GO enrichment analysis of proteins with different abundance, we found that the protein expression among ε-polylysine groups and control group may be related to cytoplasm, extracellular exosome, mitochondrion and small-subunit processome.

KEGG enriched pathways analysis of differentially abundant proteins. We used the KEGG database to map all differentially abundant proteins to further explore the effects of ε-polylysine on nutrient metabolic pathways. Top 20 KEGG pathways in 300 mg/kg group vs control group were shown in Fig. 4D, including fat digestion and absorption, PPAR signaling pathway, cholesterol metabolism, complement and coagulation cascades, phagosome, mismatch repair, proximal tubule bicarbonate reclamation, vitamin digestion and absorption, legionellosis ($P < 0.05$). The distribution diagram of up- and down-regulated differential proteins at KEGG Level2 was

KEGG pathway (Pathway ID)	Metabolites	KEGG ID	Regulation	Proteins	KEGG ID	Regulation
Glutathione metabolism (mmu00480)	Glutathione disulfide	C00127	Down	N-acetyltransferase 8 (NAT8)	Q9JIY7	Up
	Glutathione	C00051	Down	Glutathione S-transferase P 1 (GST P1)	P19157	Up
	L-Glutamate	C00025	Down			
Glycerophospholipid metabolism (mmu00564)	sn-Glycero-3-phosphocholine	C00670	Up	Lysophospholipid acyltransferase 5 (LPCAT3)	Q91V01	Down
	1-Acyl-sn-glycero-3-phosphocholine	C04230	Up/Down	Phospholipase D/5′-3′ exonuclease PLD3 (PLD3)	O35405	Up
	Phosphatidylcholine	C00157	Up	Choline/ethanolaminephosphotransferase 1 (CEPT1)	Q8BGS7	Up
	Phosphatidate	C00416	Up			
ABC transporters (mmu02010)	myo-Inositol	C00137	Down	Antigen peptide transporter 2 (TAP2)	P36371	Up
	Glutathione	C00051	Down	ATP-binding cassette sub-family G member 8 (ABCG8)	Q9DBM0	Down
	L-Glutamate	C00025	Down	Canalicular multispecific organic anion transporter 2 (cMOAT2)	B2RX12	Down
				Phospholipid-transporting ATPase ABCA1 (ABCA1)	P41233	Up

Table 8. Key pathways obtained from integrated analysis of differentially accumulated metabolites and abundant proteins.

shown in Fig. 5A. Compared 600 mg/kg group to control group, the top20 KEGG pathways included PPAR signaling pathway, pancreatic secretion, fat digestion and absorption, nicotinate and nicotinamide metabolism, purine metabolism, influenza A, complement and coagulation cascades, fluid shear stress and atherosclerosis, RNA transport, adrenergic signaling in cardiomyocytes, amyotrophic lateral sclerosis (ALS), necroptosis, glucagon signaling pathway, systemic lupus erythematosus, ribosome biogenesis in eukaryotes (Fig. 4F) ($P < 0.05$). The distribution diagram of up- and down-regulated differential proteins at KEGG Level2 was shown in Fig. 5B. The pathways, contained human papillomavirus infection, thyroid hormone signaling pathway, mRNA surveillance pathway, platinum drug resistance, autophagy, pyrimidine metabolism, AMPK signaling pathway, drug metabolism-other enzymes, spliceosome, prion diseases and toxoplasmosis, were significantly enriched ($P < 0.05$) (Fig. 4H). The distribution diagram of up- and down-regulated differential proteins between 1200 mg/kg group and control group at KEGG Level2 was shown in Fig. 5C.

Integrated analysis of the metabolome and proteome. Based on metabolomic and proteomic data, we selected the KEGG pathway as the carrier to analyze. The KEGG pathways number obtained by comparing ε-polylysine groups with the control group was shown in the Venn diagram (Fig. 6A). The cross areas in the circle represent the number of KEGG pathways involved in three ε-polylysine groups compared with the control group. We found three pathways, including glutathione metabolism, glycerophospholipid metabolism and ABC transporters (Table 8). In the glutathione metabolism pathway, the abundance of the metabolites including glutathione disulfide, glutathione and L-glutamate were decreased by ε-polylysine. In the glycerophospholipid metabolism pathway, ε-polylysine regulated the metabolites abundance of sn-glycero-3-phosphocholine, 1-acyl-sn-glycero-3-phosphocholine, phosphatidylcholine and phosphatidate, as well as, had effect on the abundance of lysophospholipid acyltransferase 5, 5′-3′ exonuclease PLD3 and choline/ethanolaminephosphotransferase 1. Furthermore, ε-polylysine decreased the metabolites abundance of myo-inositol, glutathione, L-glutamate and the proteins abundance of ATP-binding cassette sub-family G member 8, canalicular multispecific organic anion transporter 2 in the ABC transporters pathway. But, ε-polylysine increased the abundance of proteins antigen peptide transporter 2 and phospholipid-transporting ATPase ABCA1 (Table 8).

Code availability

No specific programs or codes were used in this study.

Received: 18 September 2024; Accepted: 22 April 2025;
Published online: 10 May 2025

References

1. Shima, S. *et al.* Polylysine produced by *Streptomyces*. *Agricultural and Biological Chemistry* **41**, 1807–1809 (1977).
2. Li, Y. Q. *et al.* Antibacterial characteristics and mechanisms of ε-poly-lysine against *Escherichia coli* and *Staphylococcus aureus*. *Food Control* **43**, 22–27 (2014).
3. Geornaras, I. *et al.* Activity of ε–polylysine against *Escherichia coli* O157: H7, *Salmonella Typhimurium*, and *Listeria monocytogenes*. *Journal of Food Science* **70**, M404–M408 (2005).
4. Zhang, X. *et al.* Antibacterial activity and mode of action of ε-polylysine against *Escherichia coli* O157: H7. *Journal of Medical Microbiology* **67**, 838–845 (2018).
5. Hiraki, J. *et al.* Use of ADME studies to confirm the safety of ε-polylysine as a preservative in food. *Regulatory Toxicology and Pharmacology* **37**, 328–340 (2003).
6. Lin, L. *et al.* Preparation of ε-polylysine/chitosan nanofibers for food packaging against *Salmonella* on chicken. *Food packaging and shelf life* **17**, 134–141 (2018).

7. Oppermann-Sanio, F. B. *et al*. Occurrence, functions and biosynthesis of polyamides in microorganisms and biotechnological production. *Naturwissenschaften* **89**, 11–22 (2002).
8. Yuan, J. *et al*. Preparation of self-assembled nanoparticles of ε-polylysine-sodium alginate: a sustained-release carrier for antigen delivery. *Colloids and Surfaces B: Biointerfaces* **171**, 406–412 (2018).
9. Shi, C. *et al*. ε-Polylysine and next-generation dendrigraft poly-L-lysine: chemistry, activity, and applications in biopharmaceuticals. *Journal of Biomaterials Science, Polymer Edition* **26**, 1343–1356 (2015).
10. Shukla, S. C. *et al*. Review on production and medical applications of ε-polylysine. *Biochemical Engineering Journal* **65**, 70–81 (2012).
11. Shih, L. *et al*. Microbial synthesis of poly (ε-lysine) and its various applications. *Bioresource technology* **97**, 1148–1159 (2006).
12. Zhang, X. *et al*. Dietary ε-polylysine affects on gut microbiota and plasma metabolites profiling in mice. *Frontiers in Nutrition* **9**, 842686 (2022).
13. Candiano, G. *et al*. Blue silver: a very sensitive colloidal Coomassie G-250 staining for proteome analysis. *Electrophoresis* **25**, 1327–1333 (2004).
14. Zhang, X. A multi-omics dataset of C57 BL/6J mice regulated function by feed with ε-polylysine. MMTBLS4273 http://www.ebi.ac.uk/metabolights (2024).
15. Zhang, X. The proteomic data from C57 BL/6J mice by feed with ε-polylysine. *ProteomeXchange ID PXD055010* https://www.iprox.cn/ (2024).

Acknowledgements

The present research was conducted by The Agricultural Science and Technology Innovation Program (ASTIP), Chinese Academy of Agricultural Sciences, High-level Talents Research Start-up Fund of Henan University of Technology (2022BS072), Key Research Project of Science and Technology in Colleges and Universities of Henan Province (24B230001), Henan University of Technology Open Fund Project (CSKFJJ-2025-37).

Author contributions

D.W. and X.Z. conceived the project. X.Z. and Z.H. collected samples. X.Z., Y.C.,Y.Z, and S.W. performed the experiments. X.Z. and Z.H. performed the analysis and wrote the manuscript. All authors contributed revising the manuscript and approved the final version of the manuscript.

Competing interests

The authors declare that they have no known competing financial interests or personal relationships that could have appeared to influence the work reported in this paper.

Additional information

Correspondence and requests for materials should be addressed to D.W.